AWARD NUMBER: W81XWH-08-1-0583

TITLE: Multimodal Imaging of Pathophysiological Changes and Their Role in Development of Breast Cancer Brain Metastasis

PRINCIPAL INVESTIGATOR: Dawen Zhao, M.D., Ph.D.

CONTRACTING ORGANIZATION: University of Texas Southwestern Medical Center at Dallas
Dallas, TX 75390

REPORT DATE: September 2012

TYPE OF REPORT: Final

PREPARED FOR: U.S. Army Medical Research and Materiel Command
Fort Detrick, Maryland 21702-5012

REPORT DOCUMENTATION PAGE

Form Approved
OMB No. 0704-0188

1. REPORT DATE	2. REPORT TYPE	3. DATES COVERED
1 September 2012	Final	1 Sep 2008 – 31 Aug 2012

4. TITLE AND SUBTITLE

Multimodal Imaging of Pathophysiological Changes and Their Role in Development of Breast Cancer Brain Metastasis

5a. CONTRACT NUMBER

5b. GRANT NUMBER
W81XWH-08-1-0583

5c. PROGRAM ELEMENT NUMBER

6. AUTHOR(S)

Dawen Zhao, M.D., Ph.D.

E-Mail: dawen.zhao@utsouthwestern.edu

5d. PROJECT NUMBER

5e. TASK NUMBER

5f. WORK UNIT NUMBER

7. PERFORMING ORGANIZATION NAME(S) AND ADDRESS(ES)
University of Texas Southwestern Medical Center at Dallas
Dallas, TX 75390

8. PERFORMING ORGANIZATION REPORT NUMBER

9. SPONSORING / MONITORING AGENCY NAME(S) AND ADDRESS(ES)
U.S. Army Medical Research and Materiel Command
Fort Detrick, Maryland 21702-5012

10. SPONSOR/MONITOR'S ACRONYM(S)

11. SPONSOR/MONITOR'S REPORT NUMBER(S)

12. DISTRIBUTION / AVAILABILITY STATEMENT
Approved for Public Release; Distribution Unlimited

13. SUPPLEMENTARY NOTES

14. ABSTRACT
Brain metastasis represents a poor prognosis and is frequently the cause of death in breast cancer patients. Tumor microcirculation and oxygenation play important roles in malignant progression and metastasis, as well as response to various therapies. Understanding of hypoxia development and its relationship with blood brain barrier (BBB) during intracranial tumor growth will be crucial for clinical management of breast cancer brain metastasis. We have developed a MRI approach based on an interleaved T2*- and T1-weighted MRI sequence, which will provide information of both tumor vascular and tissue oxygenation. Moreover, by introducing hypoxia reporter gene (HRE-luciferase) into breast tumor lines, we will be able to use bioluminescence imaging to monitor hypoxia initiation and development of intracranial tumors. We will also correlate BBB function based on dynamic contrast enhanced (DCE) MRI with tumor hypoxia. We believe that integration of MRI and BLI will provide temporal and spatial information of tumor hypoxia evolution. Tumor hypoxia leads to resistance to anticancer therapies, in particular radiation, which is perhaps the most important treatment modality in our current armamentarium for brain metastasis. A combination of radiation with hypoxia modifier, 2-methoxyestradiol, on brain metastases will be evaluated by in vivo imaging.

15. SUBJECT TERMS
Breast cancer brain metastasis, hypoxia, Magnetic resonance imaging, Optical imaging, irradiation

16. SECURITY CLASSIFICATION OF:			17. LIMITATION OF ABSTRACT	18. NUMBER OF PAGES	19a. NAME OF RESPONSIBLE PERSON
a. REPORT	b. ABSTRACT	c. THIS PAGE			USAMRMC
U	U	U	UU	18	19b. TELEPHONE NUMBER *(include area code)*

Table of Contents

Introduction:

Brain metastasis represents an important cause of morbidity and mortality. Clinically overt brain metastases occur in approximately 10 ~ 15% of patients with breast cancer (1, 2). The incidence of brain metastasis seems to have increased over the past decade, and may be the paradoxical result of effectiveness of drugs on primary breast cancer. Perhaps even more alarming are the growing numbers of breast cancer patients who die from complications related to brain metastasis, at a time when systemic disease is under good control. In part, this may be due to the fact that chemotherapeutic agents that show efficacy against systemic disease, may have poor penetration of the blood-brain barrier (BBB), which means that breast cancer metastasis in the brain may remain untreated and inaccessible to conventional chemotherapeutics (3-5).

Tumor microcirculation and oxygenation play important roles in malignant progression and metastasis, as well as response to various therapies. In particular, radiotherapy, and possibly some anticancer drugs, are less effective in hypoxic tumors (6, 7). There is little knowledge about tumor hypoxia during intracranial development of brain metastasis. We hypothesize that tumor hypoxia is major driving force for progression of breast cancer brain metastasis and represents a critical target for therapeutic strategies. Traditionally, pathophysiological and biological studies of brain tumor models involve sacrificing animals at different time points, and thus require a large number of animals. *In vivo* imaging promises greater efficiency since each animal serves as its own control and multiple time points can be examined sequentially. In addition to anatomic information, magnetic resonance imaging (MRI) has been increasingly applied to studying tumor pathophysiology. Blood Oxygenation Level Dependent (BOLD) MRI based on T_2^* contrast, deoxyhemoglobin, is sensitive to tumor vascular oxygenation. Recently, several studies have suggested a possibility of assessing tissue oxygenation by direct T_1 shortening due to oxygen molecule (8, 9). We have developed a MRI approach based on an interleaved T_2^*- and T_1-weighted sequence, which provides information of both tumor vascular and tissue oxygenation. Here, we plan to apply this new MRI approach to evaluating tumor hypoxia among various breast tumor lines growing intracranially.

Bioluminescence imaging (BLI), based on *in vivo* expression of luciferase, the light emitting enzyme of the firefly, is being rapidly adopted in cancer research. Luciferin, the substrate of luciferase, crosses the cell membrane and penetrates the intact BBB after injection in mice (10, 11). Several studies have demonstrated that the BLI is capable of tracking intracerebral neural cell migration (12) or monitoring intracranial tumor growth and its response to treatment (10), (13). Here, we propose to introduce a hypoxia reporter system, Hypoxia responsive element-luciferase (5HRE-luc), to various breast cancer cells. Hypoxia Inducible Factor-1alpha (HIF-1α) activity will be monitored via *in vivo* BLI by using a luciferase reporter gene under the regulation of an artificial HIF-1-dependent promoter, 5HRE (14, 15). Integration of MRI and BLI will provide temporal and spatial information of tumor hypoxia evolution.

Body:

The Statement of Work in this project had two major tasks:

Task 1. Establish mouse xenograft models of breast cancer brain metastasis and evaluate differential biological features among various breast cancer cell lines (Months 1-8):

During the 1st year period of the project, the model of breast cancer brain metastasis has been successfully established by intracranial inoculation of breast cancer cells that have been stably transfected with the hypoxia reporter gene, HRE-ODD-luc. The single nodule lesion was visualized and followed up by both BLI and MRI. As an example presented in Figure 1

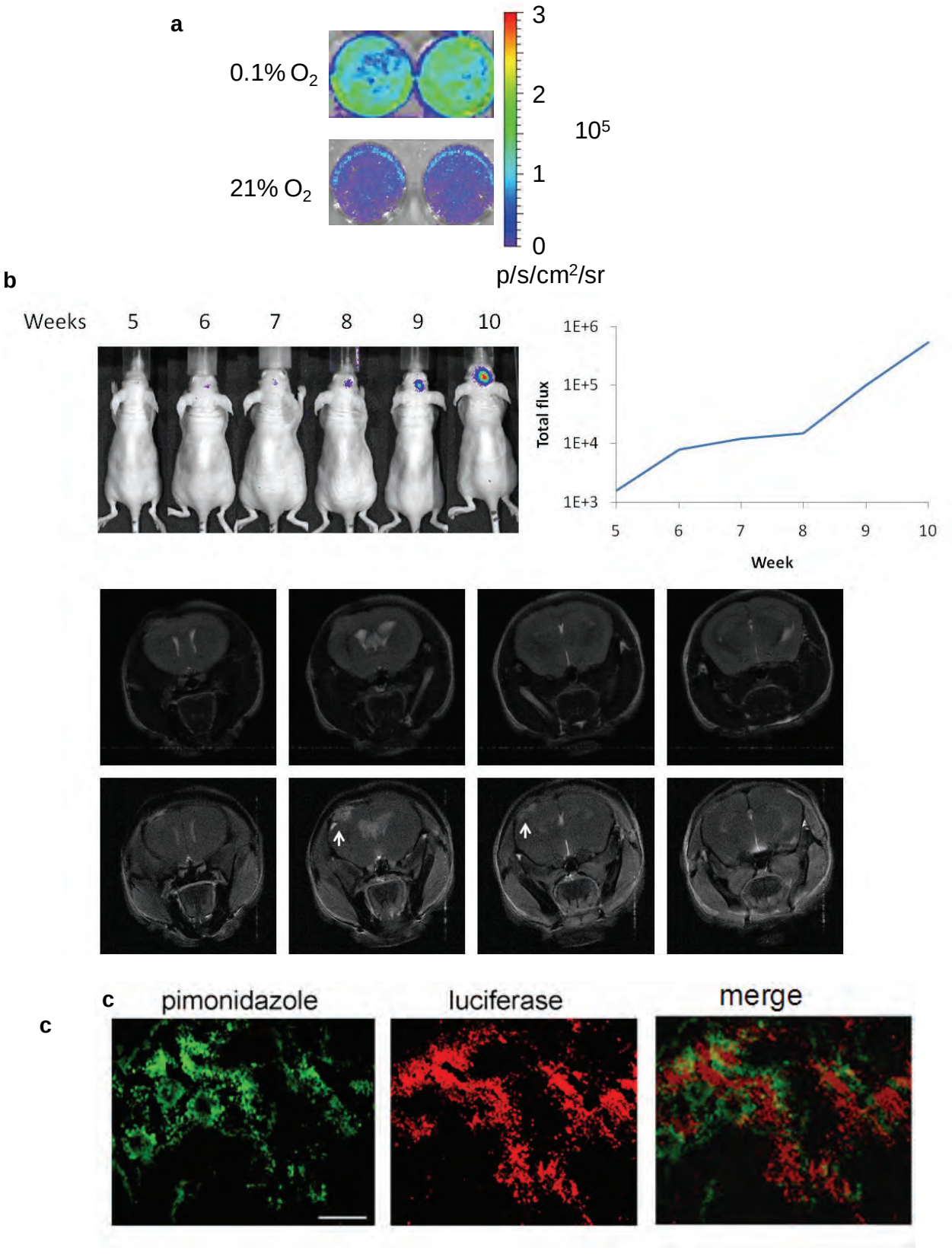
a
0.1% O2
21% O2
3
2
1
0
10^5
p/s/cm^2/sr
b
Weeks 5 6 7 8 9 10
Total flux
1E+6
1E+5
1E+4
1E+3
5 6 7 8 9 10
Week
c
pimonidazole
luciferase
merge

Fig. 1 *In vivo* detection of evolution of tumor hypoxia in MDA-MB231 cells with stable transfection of a hypoxia reporter gene, HRE-ODD-luc. a. 3×10^5 MDA-MB231/5HRE-ODD-luc cells incubated in each well of a 6-well-dish in a hypoxia chamber (0.1% O_2) for 24 hr before the medium was removed, washed and replaced with 1 ml PBS. Immediately after 100 µl luciferin was added into each well, BLI was acquired with an array of exposure times (1, 30, 60, 180 s). Strong luminescence was observed from representative wells. As a control, 3×10^5 cells incubated under normoxia (21% O_2) emitted weak light. **b.** A weak light signal from right side of mouse brain was first visualized 5 weeks after intracranial implantation of MDA-MB231/5HRE-ODD-luc breast cancer cells. Increased optical signal was observed over additional 6 weeks, indicating increased tumor hypoxia. The plot showed the time course curve of quantitative photon counts of light signal. A series of MRI T2-weighted images confirmed an intracranial tumor (arrows). **c.** A frozen mouse brain bearing a metastasis of breast cancer MDA-MB231/5HRE-ODD-luc embedded in O.C.T. was sectioned. A 10 µm section immunostained with hypoxic marker, pimonidazole, revealed intratumoral heterogeneity of hypoxia, which was found to correlate spatially with luciferase expression detected by anti-luciferase staining.

However, the direct injection approach is considered to have perturbed the normal physiological barrier in the very beginning. Thus, the data could be biased, in particular for vascular permeability analysis. To more accurately mimicking the situation of clinical cancer brain metastasis, we have created intracardiac mouse models of brain metastasis. By using ultrasound-guided left ventricular injection of brain tropic breast cancer cells, we have successfully established brain metastasis mouse models containing either a solitary (4T1 or MCF7Br) or multiple brain lesions (MDA-MB231Br).

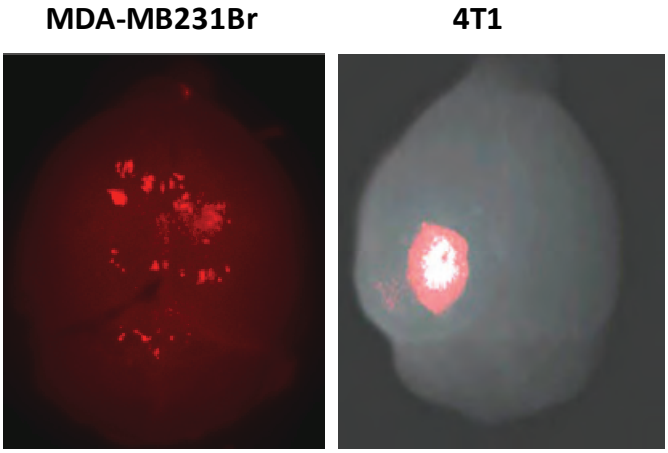

Fig. 2 Near-infrared imaging of brain metastases.
Multiple brain metastases were seen in the MDA-MB231Br model (left), while a large solitary lesion was found in a mouse receiving intracardiac injection of parental 4T1 cells (right).

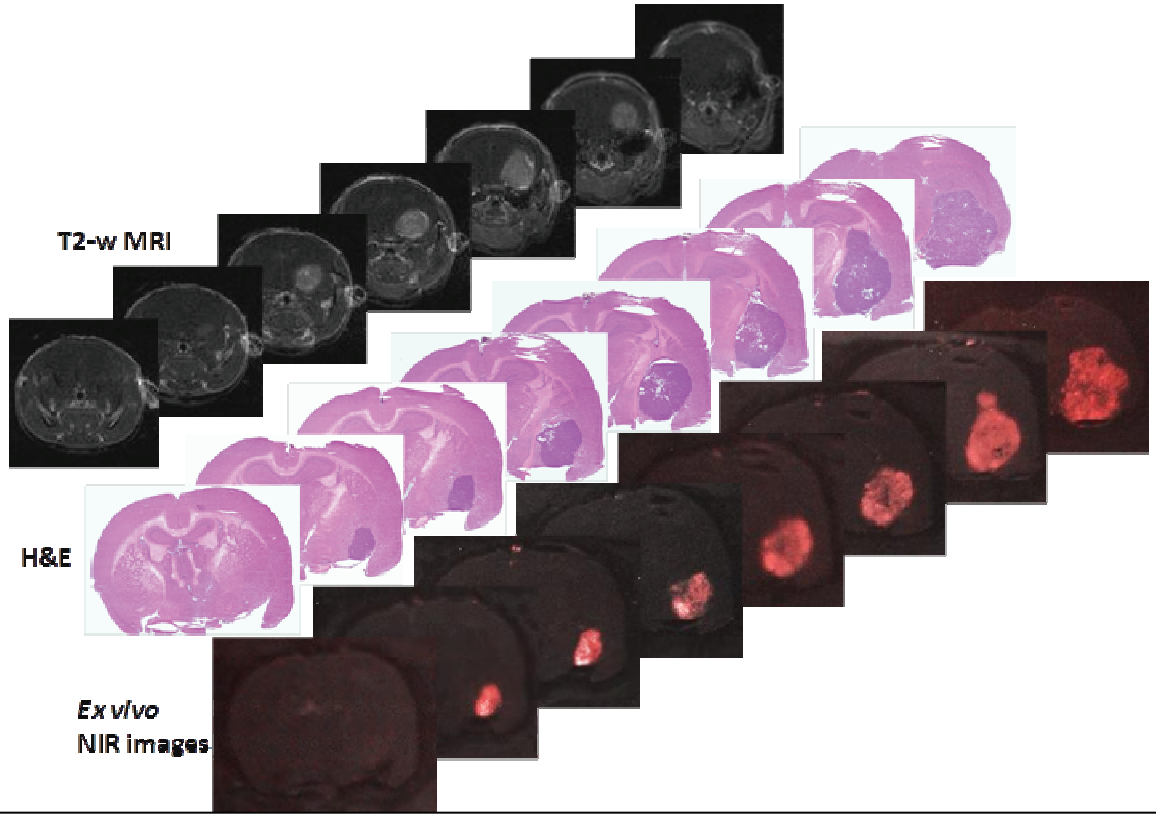

Fig. 3 A solitary brain metastasis model of 4T1 tumor. 2 x 10^5 mouse breast cancer 4T1 cells were intracardiacally injected into an immunocompetent balb/c mouse. Five weeks post injection, a solitary brain tumor was visualized on a series of T2-weighted MR images (top row), which correlated well with histological H&E staining. *Ex vivo* optical imaging clearly depicted the tumor from each of unstained frozen sections.

Fig. 4 A solitary brain metastasis model of MCF7Br. 2 x 10^5 breast cancer MCF7Br cells (provided by Dr. Steeg, NCI) were intracardiacally injected into a nude mouse. MRI scan on day 60 revealed a hyperintense brain tumor on a series of T2-weighted MR images.

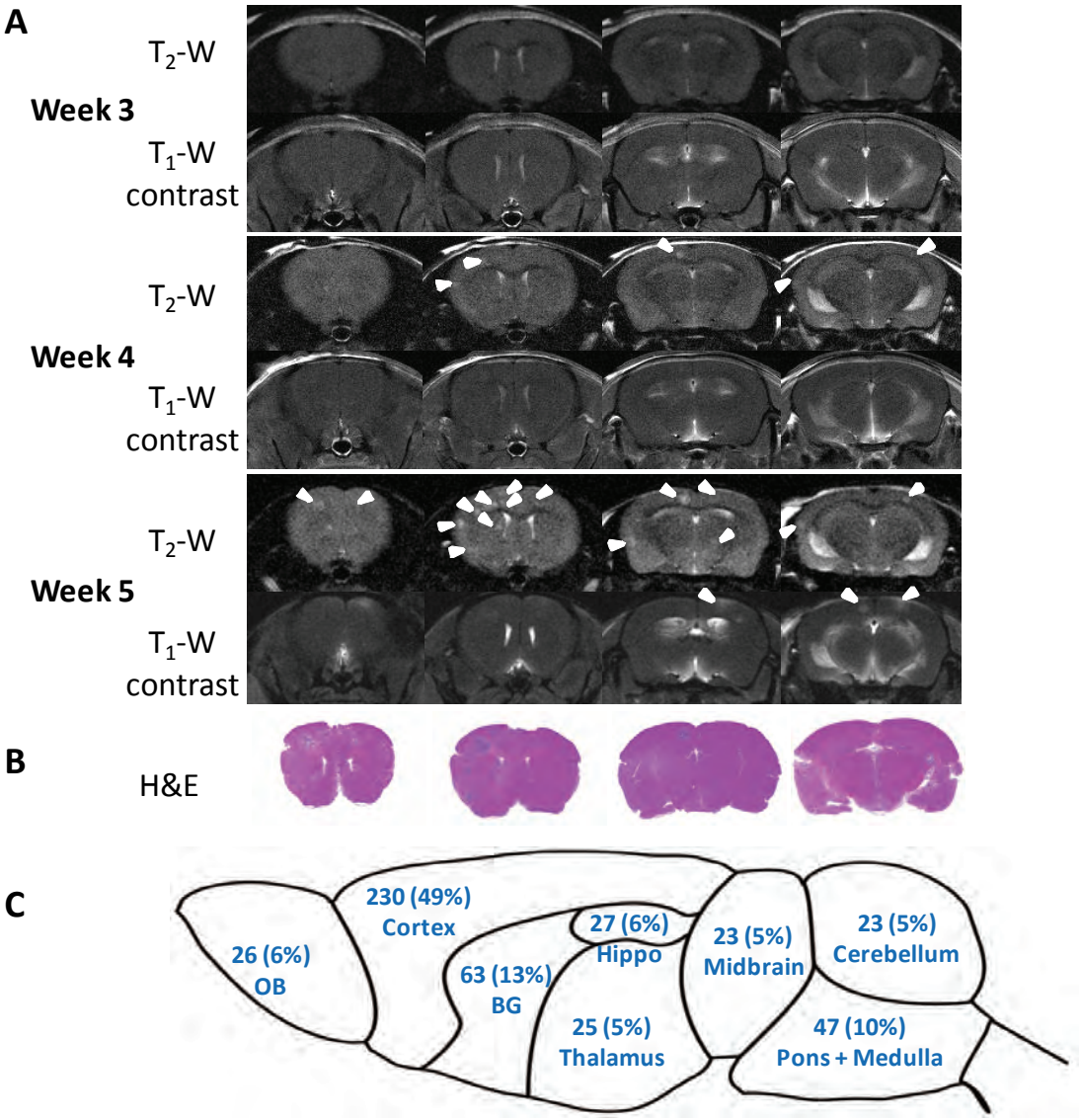

Fig. 5 A brain metastasis model bearing multiple lesions. A. Longitudinal MRI scans of the whole mouse brain were initiated 3 weeks after intracardiac injection of $2x10^5$ MDA-MB231Br cells (provided by Dr. Steeg, NCI) and repeated once a week for 2 weeks. Four consecutive coronal MRI sections of a representative mouse brain showed no apparent intracranial lesions on T_2-weighted images. However, follow-up images at week 4 identified multiple lesions with hyper-intensity on T_2-weighted images (arrowhead), but none of them was enhanced on T_1-weighted post contrast images. An increased number of lesions (arrowheads) appeared on the images at week 5, only a few of which (arrowheads) were enhanced post Gd-DTPA. **B.** Corresponding histological sections of H&E staining showed a good correlation with MRI. **C.** MRI evaluation of a total of 464 metastases in 9 mice brains indicated that these metastases distributed through the whole mouse brain with a higher incidence in the brain cortex (49%). Note: OB: Olfactory bulb; BG: Basal ganglia; Hippo: Hippocampus.

Task 2. Multimodal imaging evaluation of intracranial tumor hypoxia development and its correlation with blood brain barrier as well as aggressiveness of breast cancer brain metastasis (Months 9-24).

The major goal of this project is to integrate multiple parameters of tumor hypoxia and vasculature acquired by multimodal imaging to correlate with tumor aggressiveness and understand pathophysiological mechanism to benefit diagnosis and prognosis of clinical brain metastasis. Thus, in addition to anatomic MRI, functional MRI of studying tumor vascular and tissue oxygenation and its correlation with tumor perfusion has been initiated. Interleaved T1-weighted (TOLD) and T2*-weighted (BOLD) sequence was used to assess tumor hypoxia.

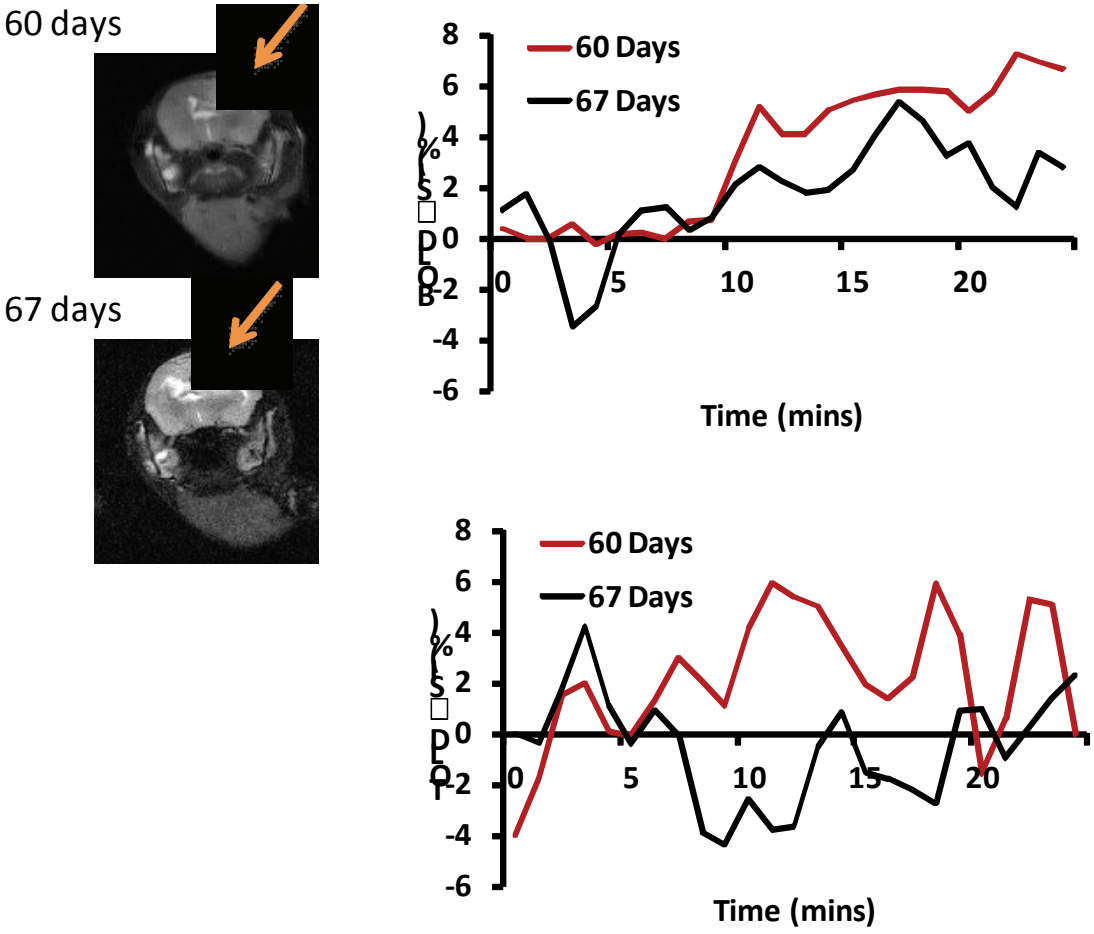

Fig. 6 BOLD and TOLD MRI of tumor hypoxia in a MCF7Br metastasis. A solitary brain metastasis was enhanced on T2-weighted MR images of day 60 and 67 post intracardiac injection. Interleaved BOLD and TOLD MRI during air and then oxygen breathing was acquired after anatomic images. Time course curves for BOLD (red) and TOLD signal changes were plotted. Maximum signal intensity change for BOLD and TOLD was 5.5% and 3.3%, respectively, on day 60. Follow up studies on day 67 showed that the change decreased to 2.9% and -0.9%, indicating that the tumor became more hypoxic.

Table 1. BOLD and TOLD MRI study of intracranial tumor hypoxia

Tumor models	Cell line	ROI	BOLD (%)	TOLD (%)
Intracranial implant	U87-luc	Tumor	5.23±5.95	5.31±4.16
		Normal	2.34±2.98	5.67±5.00
	MDA-MB-231/5HRE-ODD-luc	Tumor	1.63±1.56	5.71±3.16
		Contralateral	-2.34±2.06	6.01±3.30

Assessment of vascular properties in brain metastases is crucial for drug development and delivery. Contrast enhanced MRI and dynamic susceptibility contrast (DSC) MRI provide non-invasive interrogation of blood tumor barrier (BTB) permeability and vascular perfusion of brain metastases, respectively.

A

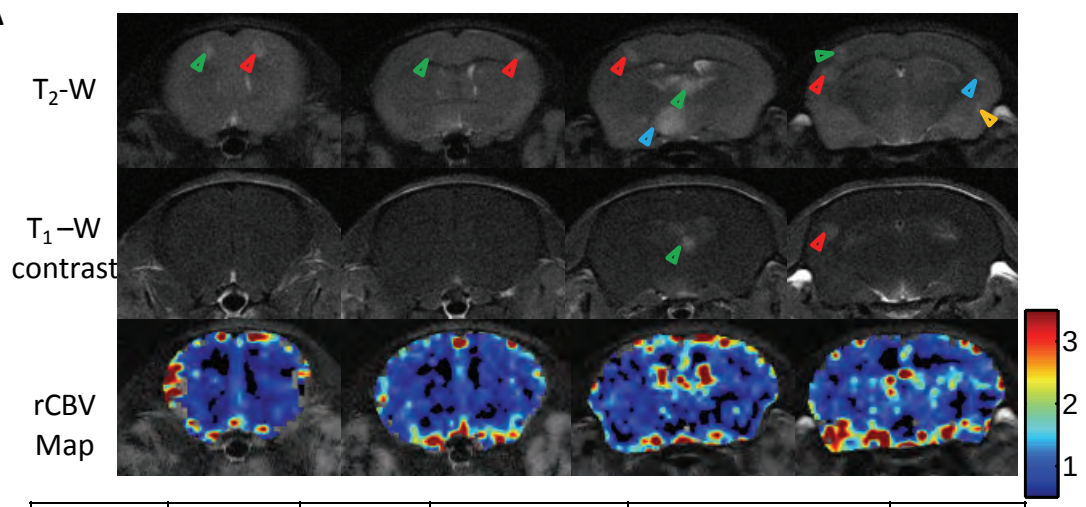

B

	slice 1		slice 2		slice3			slice4				Mean
Tumor	0.72	0.60	1.19	0.45	0.54	1.12	0.68	0.57	1.04	0.83	0.56	0.76±0.26
Contralateral	1.09	1.13	0.58	0.78	0.88	1.61	0.41	0.81	0.97	1.04	1.71	1.00±0.39

C

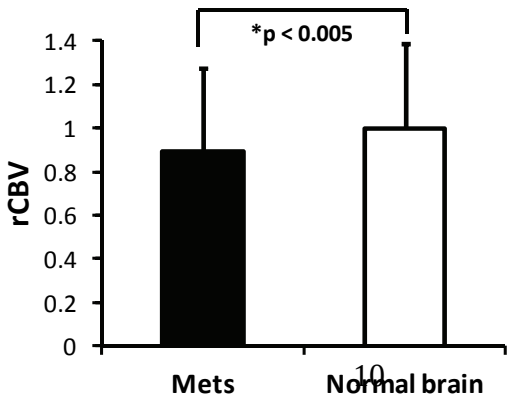

Fig. 7 Significantly lower rCBV in brain metastases than contralateral normal brain.
A. Four weeks after intracardiac injection of 231Br cells, T_2-weighted MRI revealed multiple high signal intensity lesions (arrowheads) on four consecutive coronal sections of a representative mouse brain, while only two of them (arrowheads) were enhanced on T_1-weighted post contrast images, indicating a disrupted BTB. rCBV maps of the four sections were generated and overlapped on the T_2-weighted images. **B.** The rCBV values of the metastatic lesions and their contralateral normal brain were obtained and summarized in the table. Note the color presented in the table coincides with the color of arrowhead on each of the MR images. Most of metastatic lesions had lower rCBV values than their contralateral counterparts of normal brain. **C.** Statistical analysis of rCBV in a total of 212 lesions in 9 animals obtained from the last follow-up MRI showed significantly lower rCBV of the metastatic tumors with a mean value of 0.89 ± 0.38 (s.d.), compared to the contralateral normal brain (mean = 1.00 ± 0.39; $p < 0.005$).

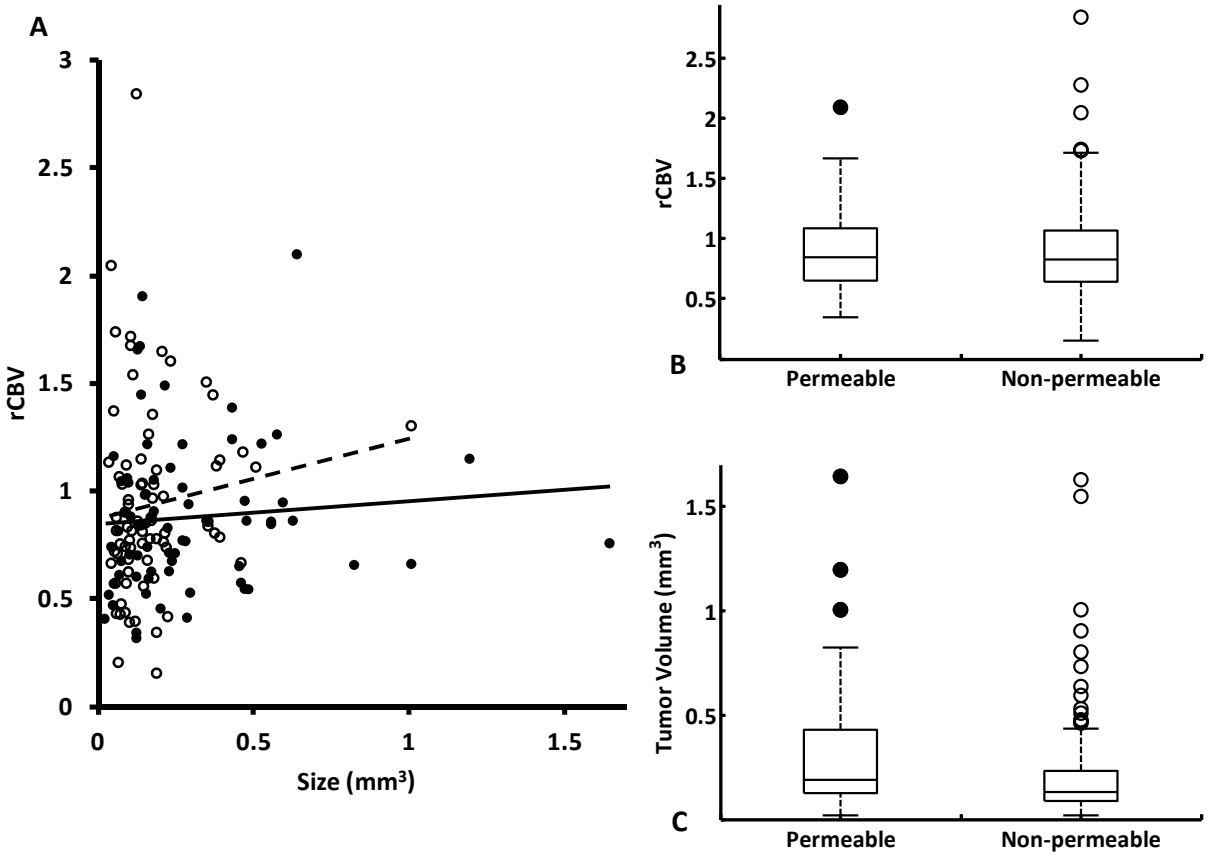

Fig. 8 Lack of correlation between rCBV, tumor size and permeability of brain metastases. Based on T_1-weighted contrast enhanced MRI, the 212 metastases studied by DSC MRI were separated into the permeable (enhanced, n = 70) and non-permeable (not enhanced, n = 142) group. **A.** A plot of rCBV versus individual tumor volume showed no correlation in either the permeable (filled; $R^2 = 0.01$) or non-permeable group (empty; $R^2 < 0.02$). **B.** The rCBV values of the permeable lesions (median = 0.84, ranging from 0.34 to 2.10) were not significantly different from those of the non-permeable ones (median = 0.82, ranging from 0.16 to 2.84; $p > 0.1$). **C.** Further comparison found no significant difference in tumor size between the permeable (mean = 0.50 ± 0.30 mm^3) and the non-permeable (mean = 0.4 ± 0.36 mm^3; $p = 0.1$) metastases.

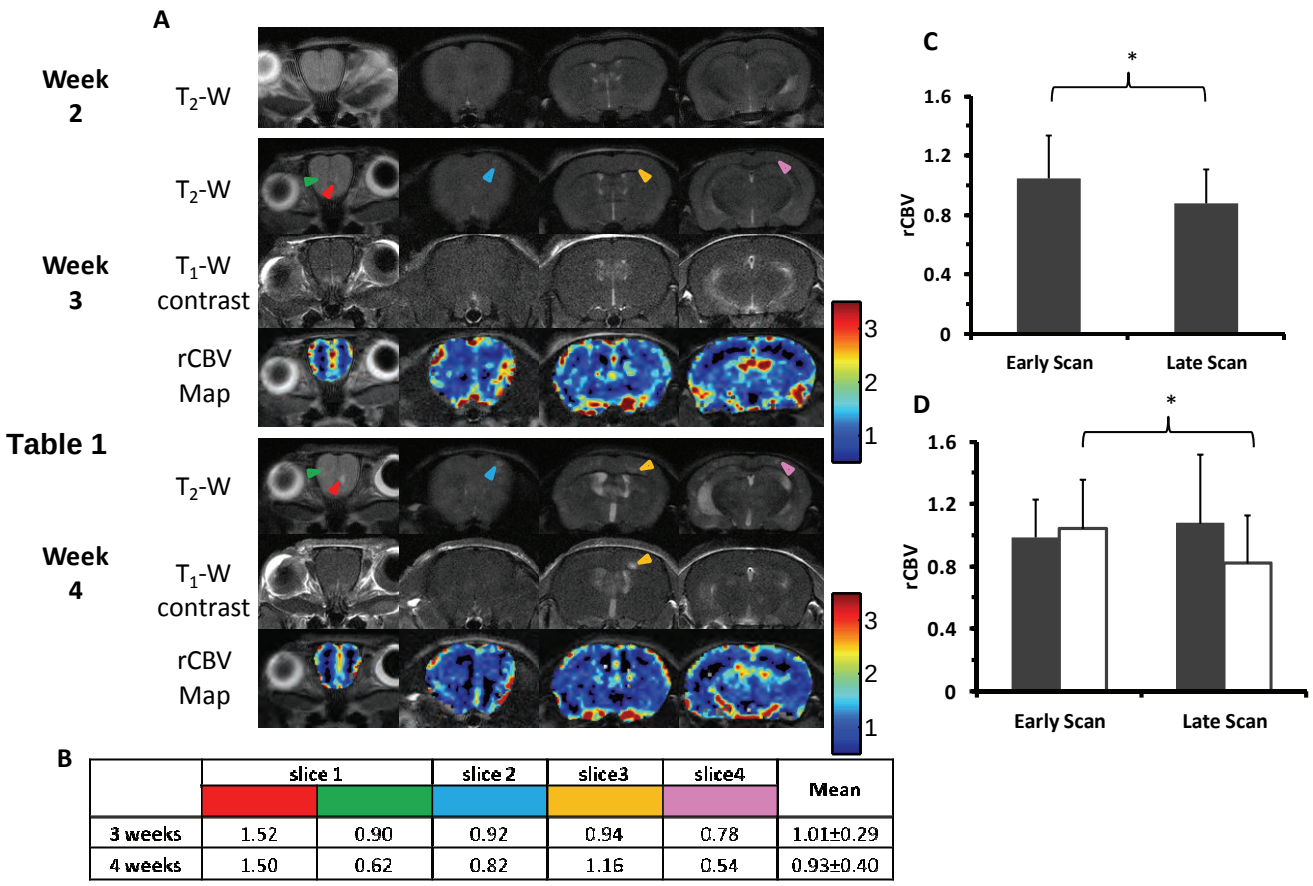

B

	slice 1		slice 2	slice3	slice4	Mean
3 weeks	1.52	0.90	0.92	0.94	0.78	1.01±0.29
4 weeks	1.50	0.62	0.82	1.16	0.54	0.93±0.40

Fig. 9 Longitudinal MRI study of changes in vascular perfusion and BTB permeability of brain metastases.

A. Longitudinal MRI of a representative mouse brain was initiated 2 weeks after intracardiac injection of 231Br cells. At week 3, five small metastases (arrowhead) were identified on four consecutive T_2-weighted coronal images. At week 4, many more lesions appeared on T_2-weighted coronal images, while all the 5 lesions seen on week 3 were found to increase in size (arrowhead). Changes in BTB permeability and vascular perfusion were then evaluated for these five lesions. There was initially no contrast enhancement seen in the five tumors at week 3, indicating an intact BTB. All the tumors except one (yellow arrowhead) still kept BTB intact at week 4. rCBV maps were created and rCBV values of the tumors were presented in the table (**B**). **C.** A total of 32 lesions in 9 animals were seen on both scans of weeks 3 and 4. Statistic analysis showed a significantly decreased rCBV at week 4 (mean = 0.88 ± 0.37) compared to week 3 (1.05 ± 0.29, $p < 0.05$). **D.** These 32 lesions were further grouped into the permeable (n = 10) and non-permeable lesions (n = 22) based on T_1-weighted contrast enhanced MRI at week 4. Comparison of rCBV between week 3 and 4 showed a significant decrease in the non-permeable tumors (mean = $p < 0.05$), while no significant change in those permeable tumors (solid, $p = 0.1$).

Our data, as shown above, clearly demonstrated that the intracardiac model can produce multiple metastatic lesions, varying in tumor size. Non-invasive MRI is capable of detecting early stage of the lesions at a size as small as < 0.2 mm and followed up their growth. These intracranial metastases were found to distribute throughout the whole brain with a preferable

site at cortex.

Table 2 Comparison of tumor vascular perfusion of the intracranial model of breast cancer brain metastasis.

Tumor models	Cell line	ROI	rCBV
Intracranial implant	U87-luc	Tumor	2.86±1.75
		Normal	1.00±0.63
	MDA-MB-231/5HRE-ODD-luc	Tumor	1.57
		Contralateral	1.00

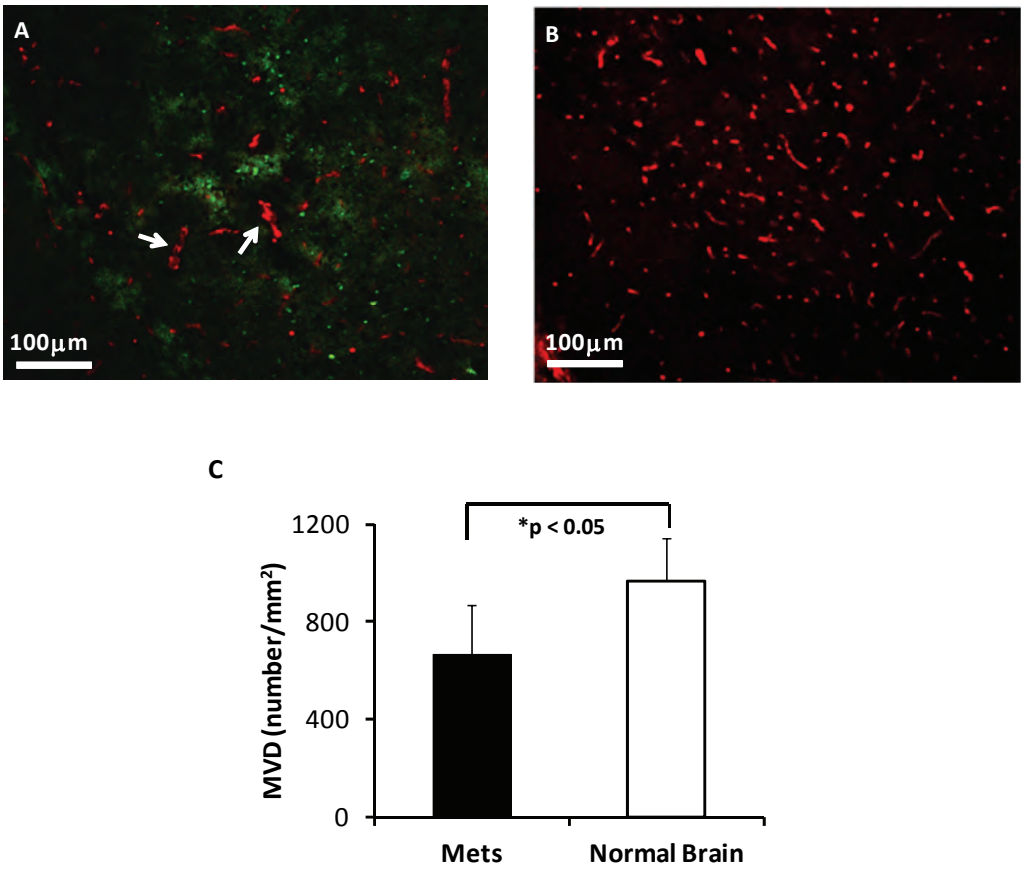

Fig. 10 Immunohistochemical study of microvascular density (MVD) in brain metastases.
A. Anti-CD31 staining was performed on a brain section bearing metastases. A relatively large lesion (~ 600 μm in diameter) was depicted with green fluorescence (GFP). Microvessels (red) within the lesion appeared less dense, as compared to abundant fine vessels in the contralateral normal brain tissues (**B**). Some of the tumor vessels were irregular in shape and larger in diameter (arrow). **C.** MVD of mets (metastases) versus contralateral normal brain showed a significantly lower MVD in brain metastases (mean = 669 ± 201/mm^2 vs. 965 ± 177/mm^2; $p < 0.05$).

In conclusion, significantly lower rCBV values were observed for brain metastases than contralateral normal brain ($p < 0.05$; Table 2), which was confirmed by histological study of tumor vascular density. In contrast, a parallel study of gliomblastoma by us found that GBM has significantly higher rCBV than contralateral normal brain. This finding, if confirmed, may have diagnostic value in terms of differential diagnosis between primary brain tumor and metastases. Comprehensive analysis suggested no significant correlation among tumor volume or tumor growth rate, rCBV and BTB permeability. Longitudinal MRI provides non-invasive assessments of spatial and temporal development of brain metastases and their vascular properties, which may have a diagnostic value.

Task 3. Evaluate brain metastasis response to a combination of chemotherapy and radiation treatment (Month 24-36).

Vigorous studies are being performed to evaluate brain metastases response to the whole brain radiation. The whole brain radiation was delivered by using small animal irradiator fitted with a variable collimator to generate a single adjustable collimated iso-dose beam of X-rays. For the brain metastases, a single dose of 10 Gy of irradiation was delivered using a D-shaped collimator to the whole brain excluding the olfactory bulb.

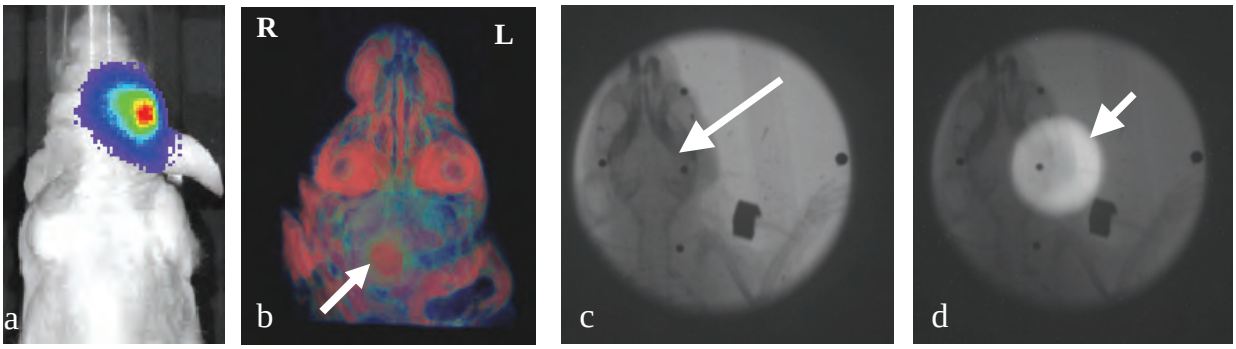

Fig. 11 Radiation treatment on brain metastasis of MDA-MB231-luc in nude mouse. Brain metastasis growing in mouse brain was observed by BLI (a). Axial MRI section of mouse brain showed an enhanced tumor in the right basal ganglia area on T1-weighted contrast enhanced 3D MRI (arrow, b). CT image acquired by CT system equipped with the small animal irradiator (X ray) indicates an axial section of mouse brain (c). A 10 Gy radiation was delivered through a 10 mm diameter collimator (arrow on overlapping image, a 5 mm diameter collimator has been built and will be used to enhance tumor targeting, d) targeting on the tumor region in right brain of the mouse.

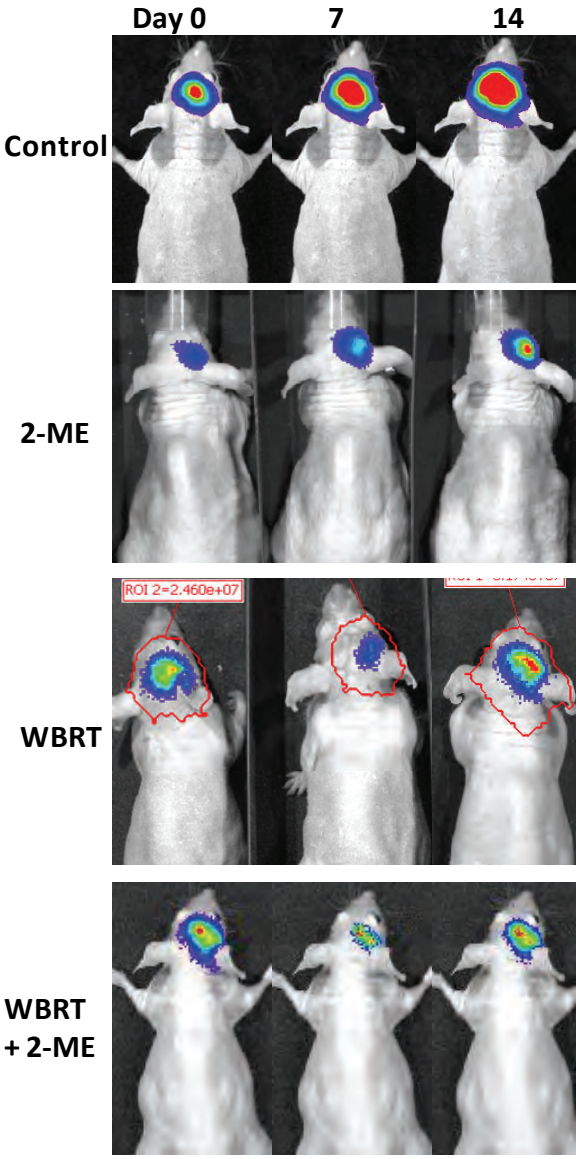

Fig. 12 BLI of a combination of 2-methoxyestradiol (2-ME) and whole brain radiation (WBRT) treatment on brain metastasis. Treatment was initiated once established brain metastasis of MDA-MB231-luc was detected by BLI. Significant intracranial tumor growth was observed in saline treated control group. 2-ME (100 mg/kg, ip, 5 doses) alone treated brain metastasis showed no significant inhibition on tumor growth. WBRT (10 Gy) inhibited initial tumor growth, but tumor re-grew by day 14. Combination of 2-ME (prior to WBRT) and WBRT showed significant inhibition of tumor growth for 14 days.

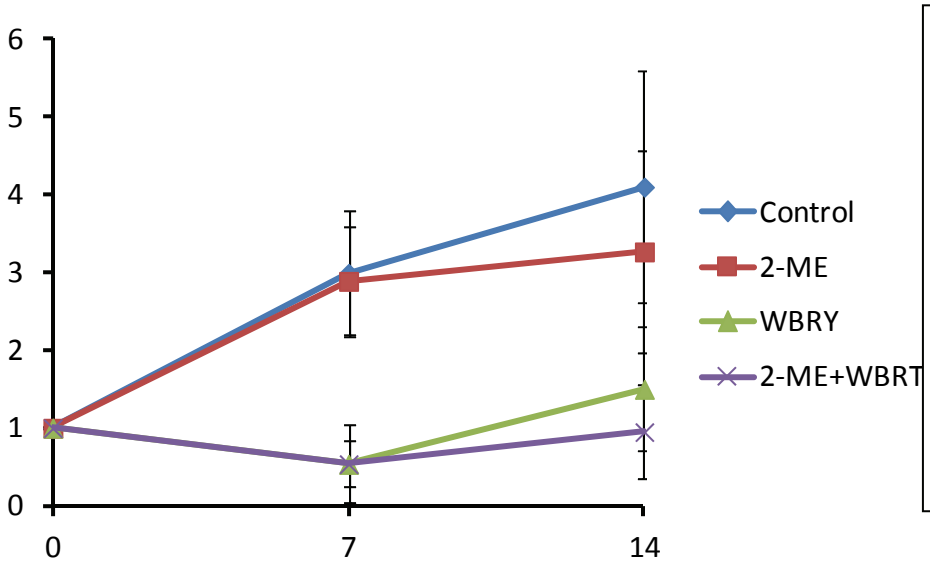

Fig. 13 BLI signal intensity time course curve following treatment. Continuous BLI signal increase was observed in control or 2-ME treated group. WBRT alone or combination of 2-ME and WBRT significantly inhibited brain metastasis growth ($p < 0.05$)

Key Research Accomplishments

- **Establishment of a new mouse model of model breast cancer brain metastasis to achieve a solitary brain metastasis, which, in combined with the model of multi-focal metastatic lesions mimic clinical brain metastasis.**

- **Successful application of in vivo BLI and MRI to study intracranial metastases distribution and monitoring their growth as well as intratumoral hypoxia development.**

- **Implement functional MRI of measuring tumor vascular perfusion rCBV.**

- **Data of rCBV show significantly lower rCBV values in brain metastases than contralateral normal brain. This finding, if confirmed, may have diagnostic value in terms of differential diagnosis between primary brain tumor and metastases.**

- **No correlation between rCBV of the metastases and tumor size, location or status of tumor BBB permeability.**

- **Histological studies confirmed characteristics of metastatic vasculature with less density and larger lumen.**

- **In vivo assessment of tumor hypoxia by BLI monitoring of the hypoxia reporter gene, HIF-1 promoted luciferase expression.**

- **In vivo MRI study of tumor oxygenation (BOLD and TOLD MRI) and correlate with tumor perfusion.**

- **Spatial correlation between these MRI parameters is performed.**

- **Design and perform whole brain irradiation (WBRT) to treat brain metastasis.**

- **Combination of 2-methoxyestradiol and WBRT significantly inhibited tumor growth of brain metastases.**

Reportable Outcomes

Publications:

Peer-reviewed paper:

Saha D, Dunn H, Zhou H, Harada H, Hiraoka M, Mason, R.P., **Zhao D**. In vivo Bioluminescence Imaging of Tumor Hypoxia Dynamics of Breast Cancer Brain Metastasis in a Mouse Model. *J Vis Exp* pii: 3175, 2011.

Published Conference Proceedings:

1) Heling Zhou, Amyn Habib, Peter Antich, Ralph P. Mason, **Dawen Zhao**. In vivo Imaging of Tumor Hypoxia and Vasculature of Orthotopic Mouse Brain Tumor

Models. Journal of Nuclear Medicine, Vol. 51, p830, 2010.

2) Heling Zhou, Amyn Habib, Peter Antich, Ralph P. Mason, **Dawen Zhao**. *In vivo* imaging of tumor hypoxia and vasculature of breast cancer brain metastasis models. *Era of Hope*, Orlando, FL, 2011.
3) Zhou, H. and **Zhao, D.** Longitudinal MRI studies of changes in tumor vascular perfusion and permeability of breast cancer brain metastasis in a mouse model. *Gordon Research Conference*, Waterville, ME, 2012.
4) **Zhao, D.,** Zhou, H., Stafford, J., Thorpe, P. Targeting phosphatidylserine enables the clear demarcation of brain metastases in mouse models. *Cell Symposium: Hallmarks of Cancer,* Accepted, San Francisco, CA, 2012.

Manuscripts preparation:

1. Zhou, H., Chen, M., Mason RP. and **Zhao, D.** Longitudinal MRI evaluation of vascular perfusion and permeability of breast cancer brain metastasis in a mouse model.
2. **Zhao, D.,** Zhou, H., Stafford, J., Thorpe, P. Phosphatidylserine-targeting antibody enables clear imaging of brain metastases in mouse models.

Employment or research opportunity:

The PhD student and research assistant, Heling Zhou, continues to work on this project.

Conclusion:

During the third year of this project, we have established a new cell line, 4T1-5HRE-ODD-luc that stably expressing luciferase under hypoxic condition. Also, a new mouse model of 4T1 breast cancer brain metastasis was established to form a solenoid brain metastatic lesion after intracardiac injection of 4T1 cells. This model, in combined with the model of multi-focal metastatic lesions, mimic clinical brain metastasis. Non-invasive BLI and MRI have been performed for early detection and tumor follow up. Functional MRI revealed characteristic vascular perfusion in these brain metastases, which may provide useful information for differential diagnosis and drug delivery. Whole brain irradiation alone or combination of 2-methoxyestradiol and WBRT significantly inhibited tumor growth of brain metastases**.** Taken together, all these baseline data have built a strong foundation for further evaluation of tumor response to therapeutics.

References:

1. Chang EL, Lo S. Diagnosis and management of central nervous system metastases from breast cancer. Oncologist 2003; 8: 398-410.
2. Gaspar L, Scott C, Rotman M, et al. Recursive partitioning analysis (RPA) of prognostic factors in three Radiation Therapy Oncology Group (RTOG) brain metastases trials. Int J Radiat Oncol Biol Phys 1997; 37: 745-51.
3. Subramanian A, Harris A, Piggott K, Shieff C, Bradford R. Metastasis to and from the central nervous system--the 'relatively protected site'. Lancet Oncol 2002; 3: 498-507.
4. Begley DJ. Delivery of therapeutic agents to the central nervous system: the problems and the possibilities. Pharmacol Ther 2004; 104: 29-45.
5. Doolittle ND, Abrey LE, Bleyer WA, et al. New frontiers in translational research in neuro-oncology and the blood-brain barrier: report of the tenth annual Blood-Brain Barrier Disruption Consortium Meeting. Clin Cancer Res 2005; 11: 421-8.
6. Brown JM, Wilson WR. Exploiting tumour hypoxia in cancer treatment. Nat Rev Cancer 2004; 4: 437-47.
7. Höckel M, Vaupel P. Tumor hypoxia: Definitions and current clinical, biologic, and molecular aspects. J Natl Cancer Inst 2001; 93: 266-76.
8. Matsumoto K, Bernardo M, Subramanian S, et al. MR assessment of changes of tumor in response to hyperbaric oxygen treatment. Magn Reson Med 2006; 56: 240-6.
9. Matsumoto S, Utsumi H, Aravalluvan T, et al. Influence of proton T1 on oxymetry using Overhauser enhanced magnetic resonance imaging. Magn Reson Med 2005; 54: 213-7.
10. Rehemtulla A, Stegman LD, Cardozo SJ, et al. Rapid and quantitative assessment of cancer treatment response using in vivo bioluminescence imaging. Neoplasia 2000; 2: 491-5.
11. Lipshutz GS, Gruber CA, Cao Y, Hardy J, Contag CH, Gaensler KM. In utero delivery of adeno-associated viral vectors: intraperitoneal gene transfer produces long-term expression. Mol Ther 2001; 3: 284-92.
12. Shah K, Bureau E, Kim DE, et al. Glioma therapy and real-time imaging of neural precursor cell migration and tumor regression. Ann Neurol 2005; 57: 34-41.
13. Jenkins DE, Hornig YS, Oei Y, Dusich J, Purchio T. Bioluminescent human breast cancer cell lines that permit rapid and sensitive in vivo detection of mammary tumors and multiple metastases in immune deficient mice. Breast Cancer Res 2005; 7: R444-54.
14. Harada H, Kizaka-Kondoh S, Hiraoka M. Optical imaging of tumor hypoxia and evaluation of efficacy of a hypoxia-targeting drug in living animals. Mol Imaging 2005; 4: 182-93.
15. Harada H, Kizaka-Kondoh S, Hiraoka M. Mechanism of hypoxia-specific cytotoxicity of procaspase-3 fused with a VHL-mediated protein destruction motif of HIF-1alpha containing Pro564. FEBS Lett 2006; 580: 5718-22.